



Nuo Chen

Department of Atmospheric and Oceanic Sciences, University of Wisconsin-Madison

Background and Motivation

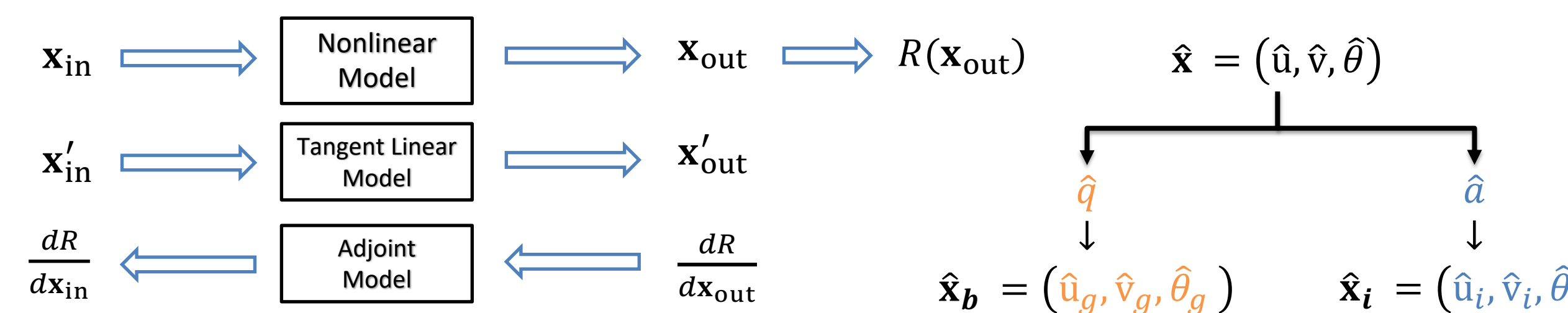
Combining the adjoint sensitivity to winds and to temperature into the sensitivity to potential vorticity (PV) provides a clear dynamical insight into extratropical cyclone development. However, in many extreme and unpredictable events, the secondary circulation leaves much sensitivity unexplained by the quasi-geostrophic (QG) assumption. Here we seek to explain the intensification of the 1998 November witch storm by partitioning the adjoint sensitivity from the Weather Research and Forecasting (WRF) model version 3.8 into geostrophically balanced and unbalanced components.

The goals of this poster include:

1. Explaining the physical meaning of geostrophic imbalance and the sensitivity to imbalance;
2. Diagnosing and describing the sensitivities to geostrophic balanced and unbalanced field leading to the deepening of the 1998 November witch storm.

Adjoint sensitivity

Any forecast aspect (response function R) is a function of state vectors $R(\mathbf{x}) = R(u, v, p, T, q_p)$. Change in R can be expressed as: $dR = dR/d\mathbf{x} \cdot \delta\mathbf{x}$. Define the adjoint sensitivity: $\hat{\mathbf{x}} = dR/d\mathbf{x}$



Sensitivity to PV and to imbalance

Define QGPV and the deviation from the geostrophic balance as:

Following Arbogast (1998) the sensitivity to QGPV (\hat{q}) and sensitivity to geostrophic imbalance (\hat{a}) are

Adjoint sensitivity to geostrophically balanced states from

$$q' = \frac{\partial u_g}{\partial x} - \frac{\partial u_g}{\partial y} - \frac{\partial}{\partial p} \left(\frac{f_0}{S} \gamma \theta' \right) \rightarrow \hat{u}_g = \frac{\partial \hat{q}}{\partial y}; \hat{v}_g = -\frac{\partial \hat{q}}{\partial x}; \hat{\theta}_g = \frac{f_0 \gamma}{S} \frac{\partial \hat{q}}{\partial p}$$

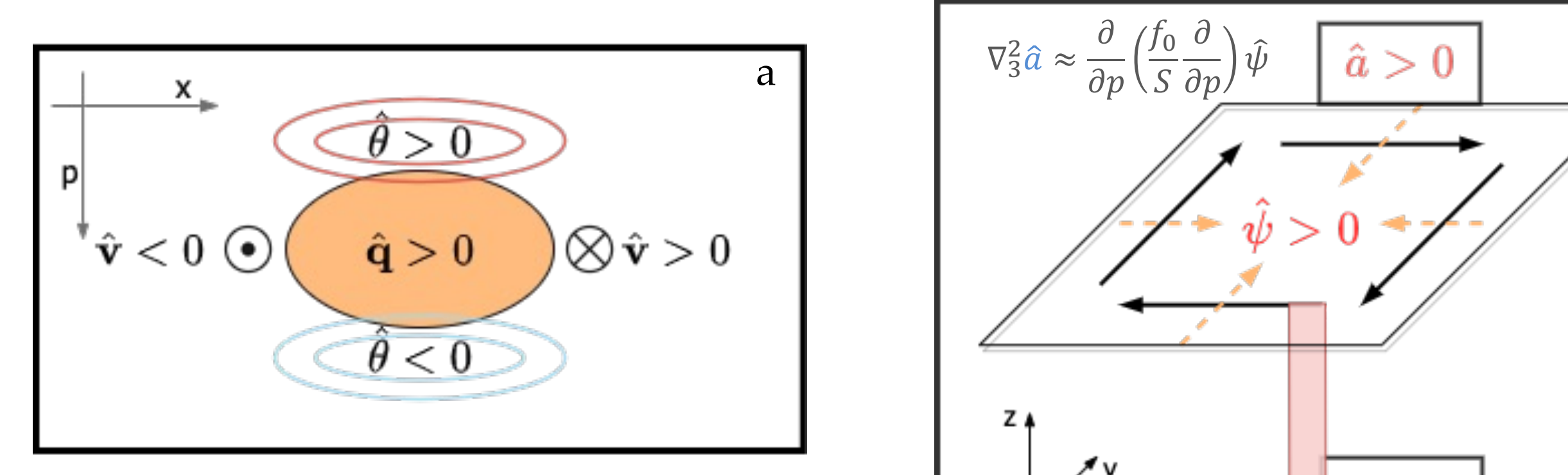


Figure 1: Schematics of a) sensitivity to QGPV \hat{q} and to geostrophically balanced states \hat{v}_g and $\hat{\theta}_g$, b) sensitivity to geostrophic imbalance \hat{a} and its associated stream function/wind component – solid arrow for instantaneous wind sensitivity and dash arrow depicts wind sensitivity after geostrophic adjustment, c) sensitivity to geostrophic imbalance \hat{a} and its associated geopotential/temperature component – brown convex shows a preference for lower geopotential, while blue concave shows a preference for higher geopotential. The red arrow shows a tendency of the sensitivity to downward vertical motion with a positive imbalance above and negative imbalance below.

✓ The similarity between the PV anomaly structure and the sensitivity to PV structure (cyclonic winds around with warm sensitivity above and cold sensitivity below) encourages one to think of adjoint sensitivity as how the atmosphere responds when putting in a perturbation.

✓ Wind associated with the imbalance is the rotational part of the ageostrophic winds $k \times \nabla a' = k \times \nabla \psi' - \frac{1}{f_0} k \times \nabla \phi' = \vec{v}_r - \vec{v}_g$

✓ Taking the divergence of the linearized shallow water equation gives $\partial \delta / \partial t = f \zeta - \nabla^2 \phi'$ and $\partial \chi' / \partial t = f(\psi' - \phi'/f) = fa$, which reveals the relationship between divergence and time tendency of imbalance. This relationship allows us to derive sensitivity to vertical motion from the time tendency of sensitivity to imbalance: $\hat{a} = \nabla^{-2} \frac{\partial}{\partial p} \left(-\frac{1}{f} \frac{\partial \hat{a}}{\partial t} \right)$

Case Study

The 1998 November Witch Storm caused intense convective precipitation from the Midwest to the southern plains, as well as sustained surface winds in excess of 40 knots in Wisconsin and Minnesota. The storm rapidly developed from 996 hPa on Nov 10 00z to 967 hPa on Nov 11 00z.

WRF simulation was carried out with $\frac{1}{4}$ degree GFS FNL reanalysis, 24km grid spacing and 41 vertical levels from Nov 09 18z (F00) to Nov 10 18z (F24).

To investigate which features intensified the storm at F24, we let the response function be the column dry air mass ($R = -\hat{a}'$) within the 980 hPa contour at F24, and let WRFPLUS V3.8 carry the adjoint integration backward in time

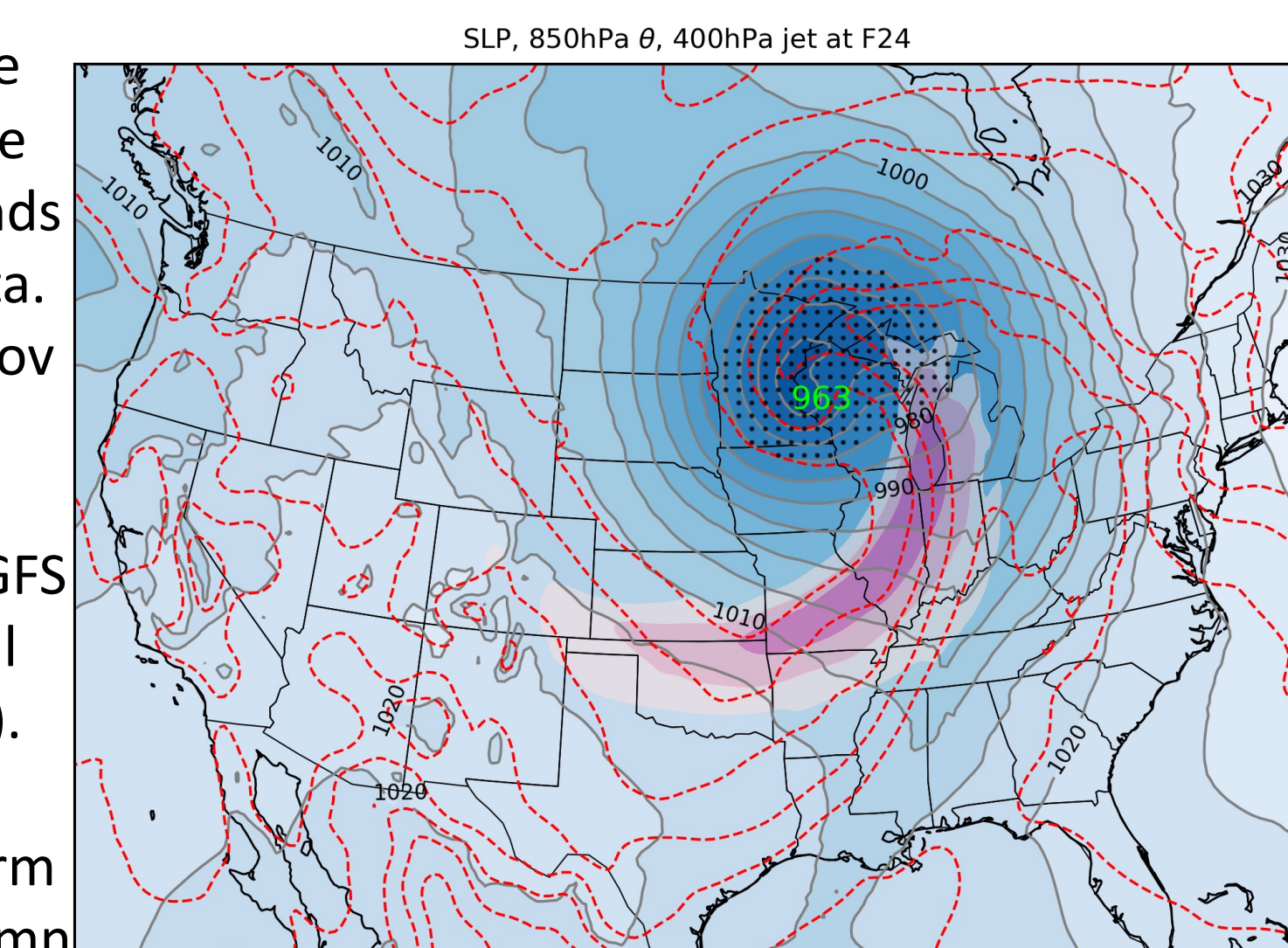


Figure 2: Final time SLP (gray contour), potential temperature (red dashed), jet (pink shading), response function area (meshed)

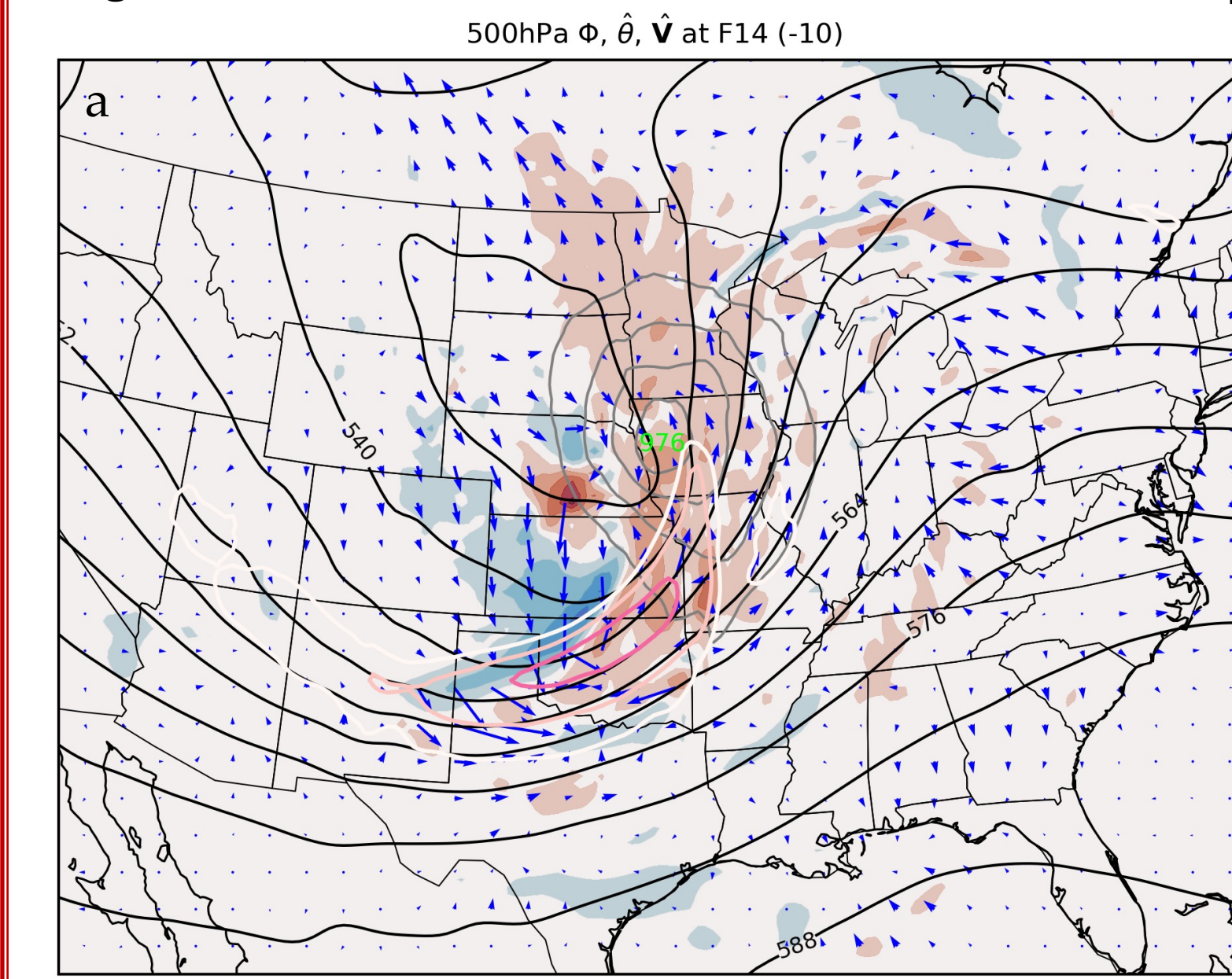


Figure 3: F14 a) 500hPa sensitivity to winds from wrfplus (blue arrow), sensitivity to potential temperature (shaded), background geopotential height (black contour) and jet (pink contour); b) sensitivity to QGPV (positive in orange contour), sensitivity to geostrophically balanced winds (blue arrow), sensitivity to imbalance (shaded), background Ertel PV (black contour).

Unbalanced temperature and vertical motion

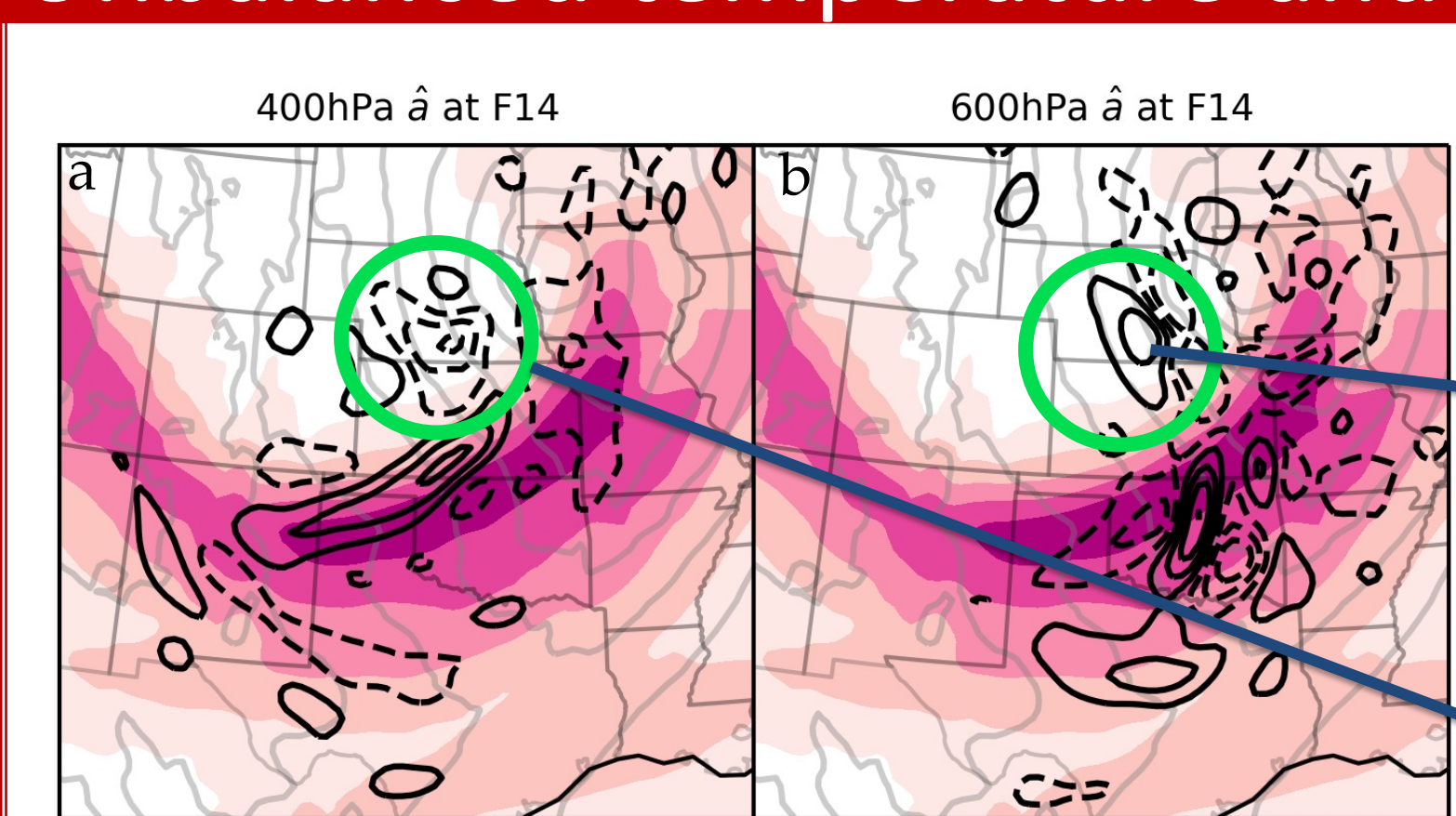


Figure 4: 300 hPa jet (shaded) and sensitivity to imbalance \hat{a} (contour) on a) 400 hPa and b) 600 hPa.

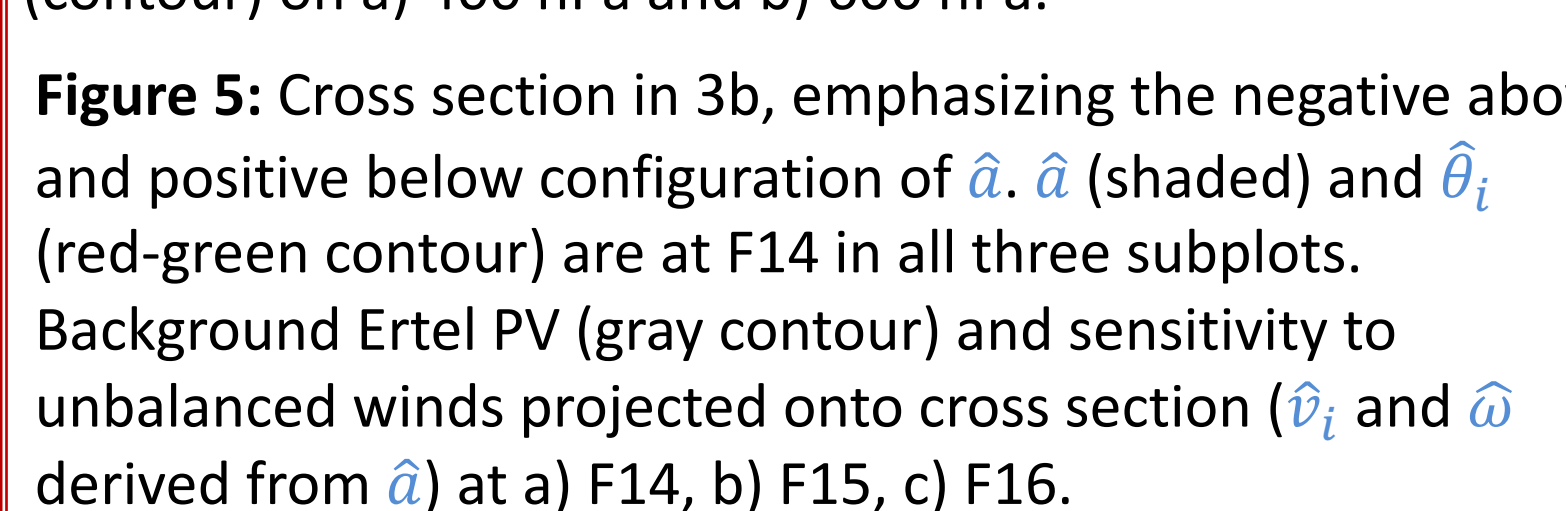


Figure 5: Cross section in 3b, emphasizing the negative above and positive below configuration of \hat{a} (\hat{a} shaded) and $\hat{\theta}_i$ (red-green contour) are at F14 in all three subplots. Background Ertel PV (gray contour) and sensitivity to unbalanced winds projected onto cross section (v_i and ω) derived from \hat{a} at a) F14, b) F15, c) F16.

✓ Sensitivity to warm air is posed between when there is negative \hat{a} above and positive \hat{a} below.

In geostrophic adjustment theory, when there is a warm air perturbation, the atmosphere will respond with adiabatic cooling manifested by upward vertical motion. At F15, we see sensitivity to ascending air with warm sensitivity and sensitivity to descending air with cold sensitivity. This relationship requires time to respond, which is why the signals are not as strong at F14 or F16. A warm sensitivity is likely to be associated with latent heat release (Fig 6d), and contributes to deepening the trough of warm air aloft (Martin 1998).

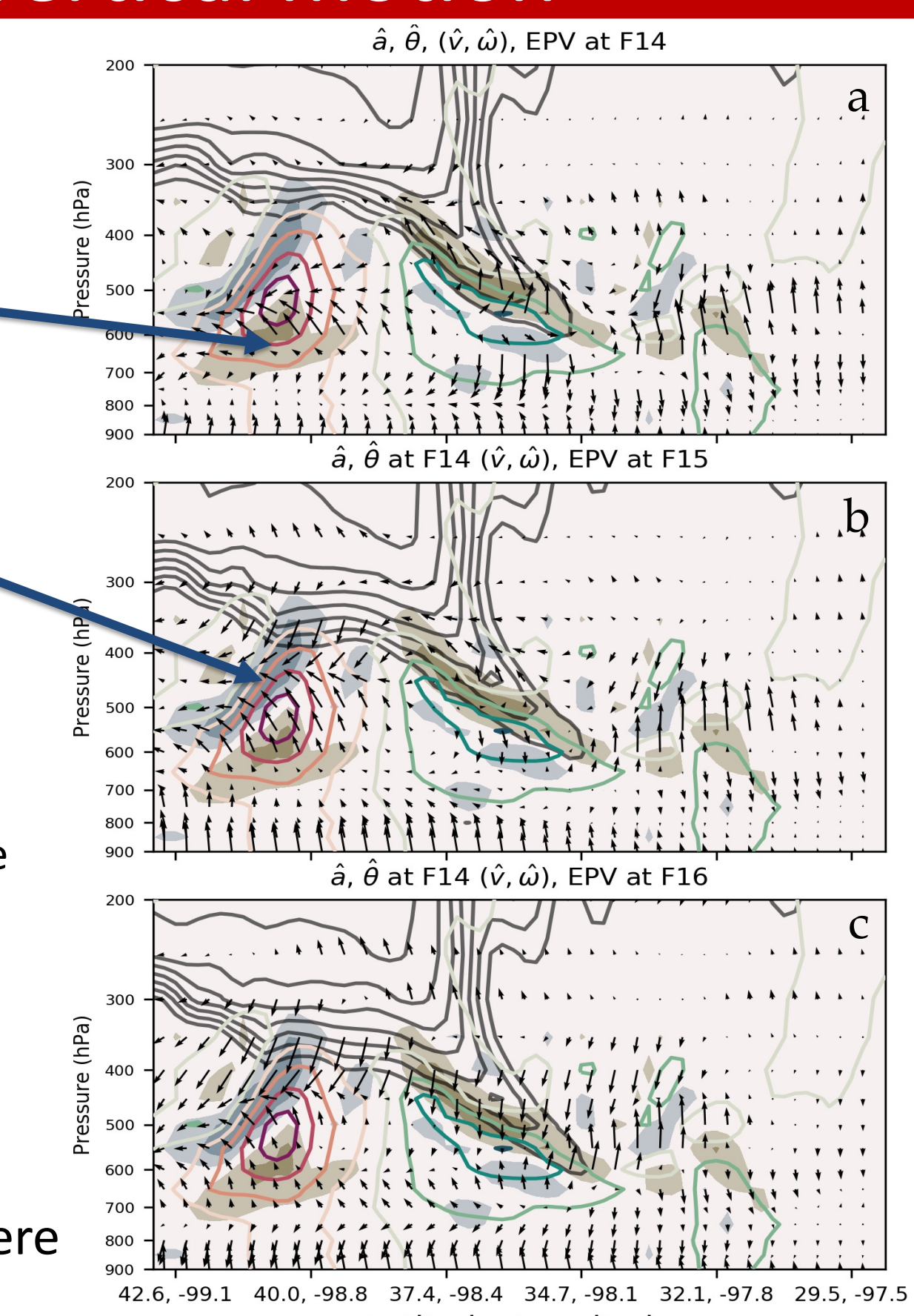


Figure 6: Cross sections of a) sensitivity to QGPV \hat{q} (orange/purple shading), sensitivity to geostrophically balanced potential temperature $\hat{\theta}_g$ (red/blue shading), to geostrophically balanced winds \hat{v}_g (barbs) and background Ertel PV (green contour); b) sensitivity to imbalance \hat{a} (brown/blue shading), unbalanced component of sensitivity to potential temperature $\hat{\theta}_i$ (red/blue shading) to unbalanced winds \hat{v}_i (barbs), background jet core (pink contour) and potential temperature (gray contour); c) sensitivity to zonal wind from wrfplus (shading), geostrophically balanced component (black contour), unbalanced component (blue contour); d) sensitivity to potential temperature from wrfplus (shading), geostrophically balanced component (black contour), unbalanced component (blue contour), and accumulated non-convective precipitation (orange line).

✓ A positive sensitivity to QGPV (Fig. 6a) suggests intensifying PV on the cyclonic side of the jet at F14 is favorable for storm development. The unbalance component to temperature (Fig. 6b) suggests a steeper north-south potential temperature gradient (thus stronger jet and higher PV) is required for the storm to deepen.

✓ Fig. 6c suggests that \hat{u}_g inverted from \hat{q} explains most of the total \hat{u} from the model output, while Fig. 6d suggests that $\hat{\theta}_i$ inverted from \hat{a} explains most of the total $\hat{\theta}$ from the model output. At the same time, strong warm sensitivity north to the jet is likely associated with stratiform precipitation.

Conclusions

1. Sensitivity to QGPV \hat{q} and to imbalance \hat{a} combines different sensitivities, making it easier to understand the dynamical aspects leading to cyclone development;
2. Unbalanced component of sensitivity to potential temperature $\hat{\theta}_i$ explains most of the temperature sensitivities, while geostrophically balanced sensitivity to winds \hat{v}_g dominates the wind sensitivities;
3. Unbalanced component of sensitivity to potential temperature $\hat{\theta}_i$ inverted from sensitivity to imbalance \hat{a} is likely to be related to the latent heat release;
4. Since geostrophic balance constrains the QGPV inversion, sensitivity to imbalance has the potential to explain the sensitivity to vertical motion with geostrophic adjustment argument;
5. Although the \hat{q} and \hat{a} are analyzed around the jet, they are also effective when analyzing the sensitivity to temperature and to winds upstream and downstream of the surface front.

Reference

- Arbogast, P., 1998: Sensitivity to potential vorticity. *Quart. J. Roy. Meteor. Soc.*, **124**, 1605–1615.
Martin, J. E., 1998: The Structure and Evolution of a Continental Winter Cyclone. Part I: Frontal Structure and the Occlusion Process. *Mon. Wea. Rev.*, **126**(2), 303–328.

Acknowledgements

This study is supported by the Space Science Engineering Center/Cooperative Institute for Meteorological Satellite Studies. The author appreciates suggestions by Dr. Jonathan Martin and Dr. Michael Morgan.